

Same-sign Charged Higgs Pair Production in bosonic decay channels at the HL-LHC and HE-LHC



Chih-Ting Lu
(KIAS)

Collaborators :
Abdesslam Arhrib, Kingman Cheung
Ref : arXiv:1910.02571

**NCTS Annual Theory Meeting 2019:
Particles, Cosmology and Strings**

NCTS

December 12th-14th, Hsinchu



Contents

- 1. Motivation
- 2. Brief review of 2HDM's
- 3. Constraints on 2HDM's
- 4. Same-sign charged Higgs pair production
- 5. Conclusions

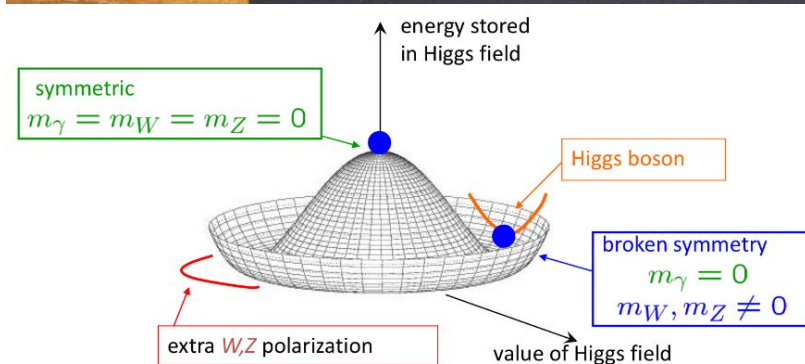
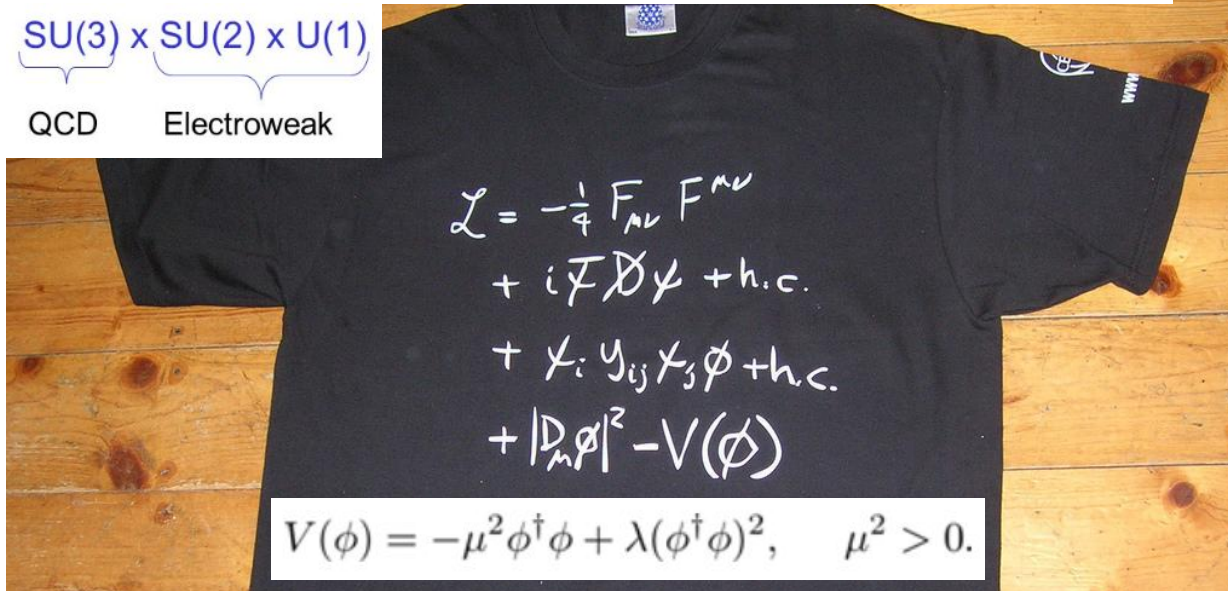
Contents

- **1. Motivation**
- 2. Brief review of 2HDM's
- 3. Constraints on 2HDM's
- 4. Same-sign charged Higgs pair production
- 5. Conclusions

Motivation : Incredible Success of the Standard Model

The Absolutely Amazing Theory of Almost Everything.

$SU(3) \times SU(2) \times U(1)$
QCD Electroweak



Standard Model of Elementary Particles

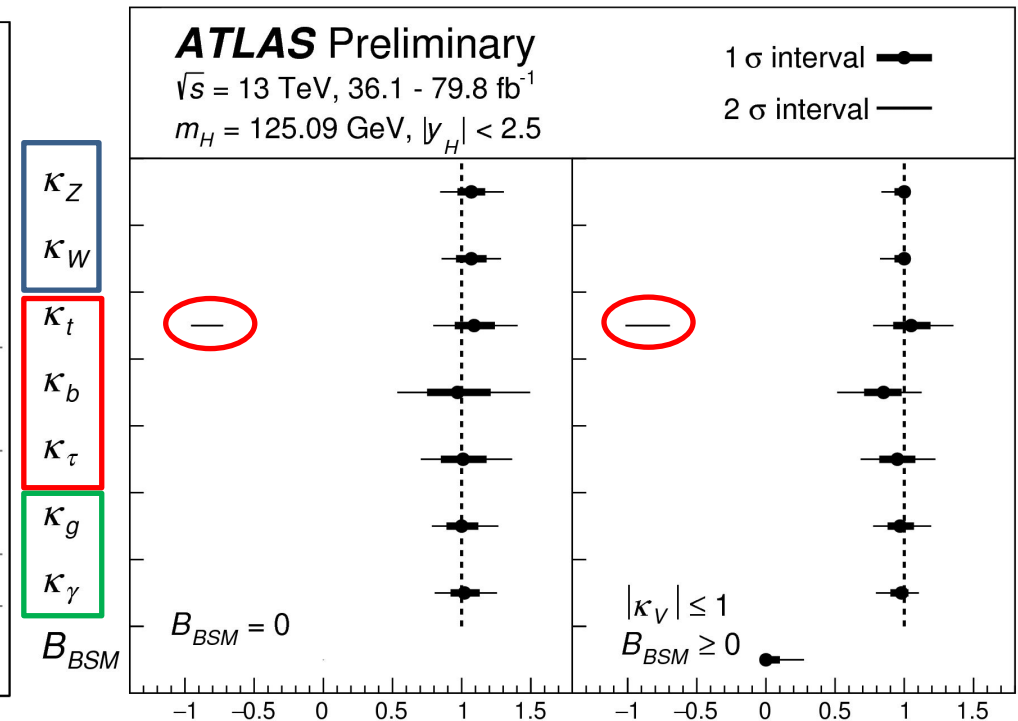
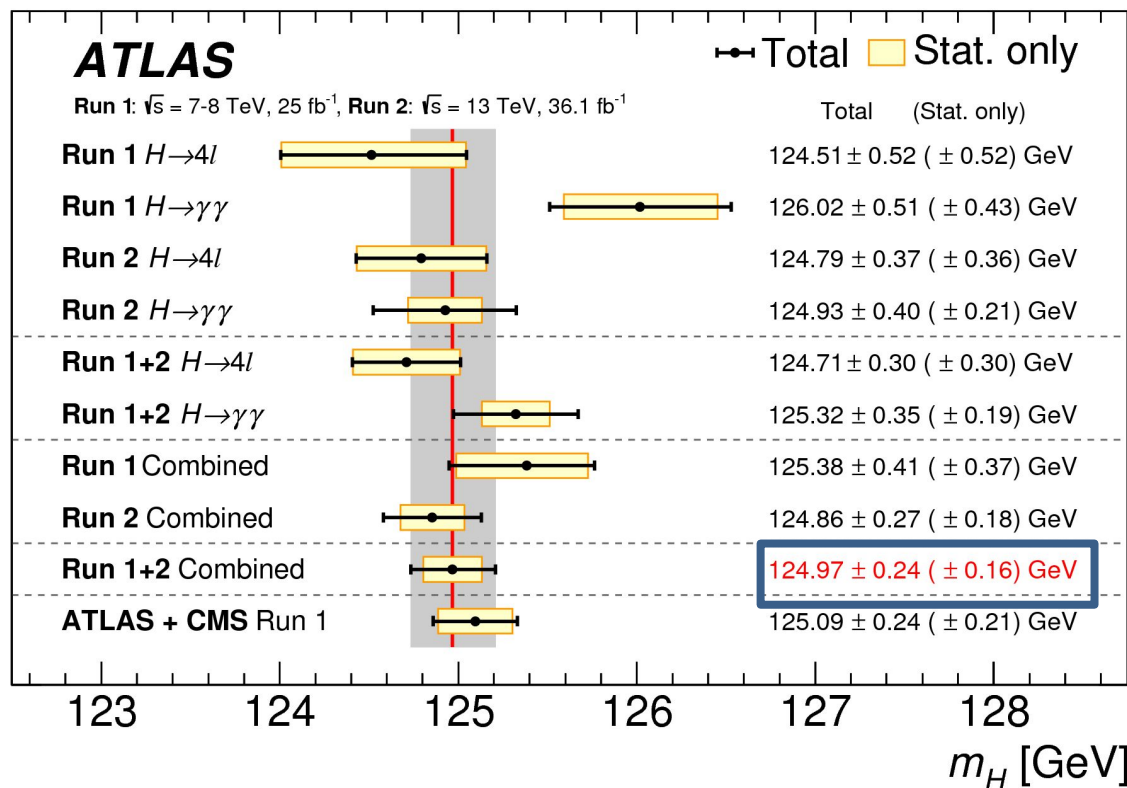
three generations of matter (fermions)					
I		II		III	
mass charge spin	$\approx 2.2 \text{ MeV}/c^2$ $2/3$ $1/2$	$\approx 1.28 \text{ GeV}/c^2$ $2/3$ $1/2$	$\approx 173.1 \text{ GeV}/c^2$ $2/3$ $1/2$	0 0 1	$\approx 125.09 \text{ GeV}/c^2$ 0 0 0
	u up	c charm	t top	g gluon	H Higgs
QUARKS	$\approx 4.7 \text{ MeV}/c^2$ $-1/3$ $1/2$	$\approx 96 \text{ MeV}/c^2$ $-1/3$ $1/2$	$\approx 4.18 \text{ GeV}/c^2$ $-1/3$ $1/2$	0 0 1	
	d down	s strange	b bottom	γ photon	
	$\approx 0.511 \text{ MeV}/c^2$ -1 $1/2$	$\approx 105.66 \text{ MeV}/c^2$ -1 $1/2$	$\approx 1.7768 \text{ GeV}/c^2$ -1 $1/2$	0 1 1	
LEPTONS	e electron	μ muon	τ tau	Z Z boson	
	$< 2.2 \text{ eV}/c^2$ 0 $1/2$	$< 1.7 \text{ MeV}/c^2$ 0 $1/2$	$< 15.5 \text{ MeV}/c^2$ 0 $1/2$	$\approx 80.39 \text{ GeV}/c^2$ ± 1 1	
	ν _e electron neutrino	ν _μ muon neutrino	ν _τ tau neutrino	W W boson	
				SCALAR BOSONS	
				GAUGE BOSONS	

Fig. 1: Particle content of the Standard Model. Courtesy to Wikipedia.



The mission of the new LHC run at 14 TeV

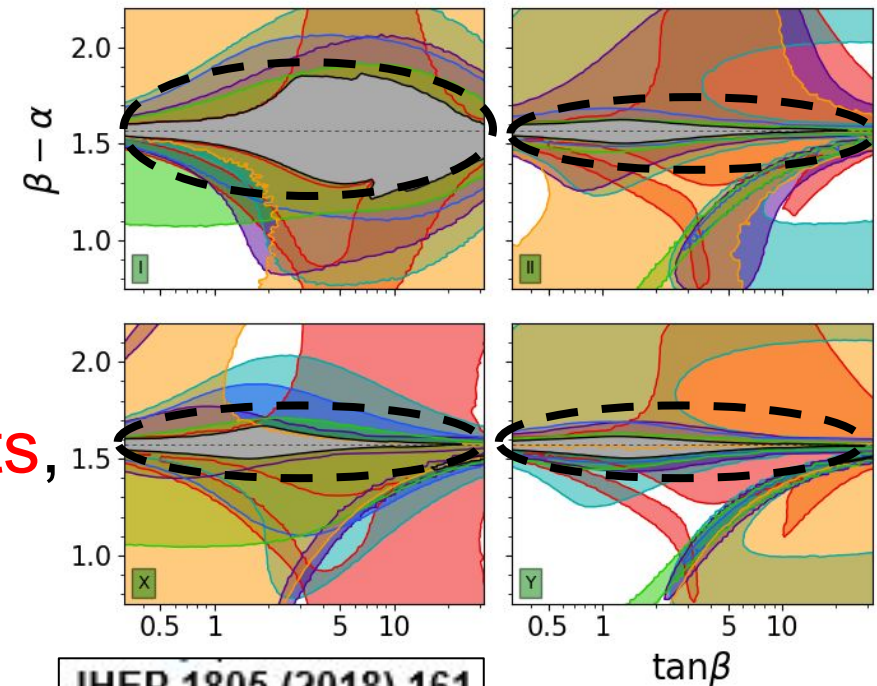
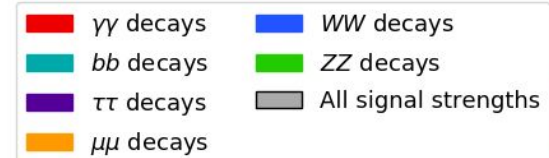
- The first task is the improvement of the scalar boson mass and scalar boson coupling measurements.



The mission of the new LHC run at 14 TeV

Accurate measurements of the scalar boson couplings to the SM particles would be helpful to determine if the Higgs-like particle is indeed the SM Higgs boson or a Higgs boson that belongs to a higher representation, such as models with **extra Higgs doublets**, **extra triplets**, or **singlets**.

Two-Higgs-Doublet Model Fits



JHEP 1805 (2018) 161

The mission of the new LHC run at 14 TeV

- The second task is to find a clear hint of new physics.
- Non-minimal Higgs sector models can explain the observed Higgs-like particle and account for some weakness of the SM.
- One common feature of many extensions of the presence of **extra neutral Higgs bosons** as well as **singly-charged Higgs bosons** in the physical spectrum.
- Therefore, the discovery of these extra bosons, especially for **charged Higgs boson** would be an unambiguous sign of physics beyond the SM.

Charged Higgs boson productions at hadron colliders

- 1. Production from top decay : $pp \rightarrow t\bar{t} \rightarrow t\bar{b}H^-$
- 2. Single charged Higgs production :
- (QCD processes : $gb \rightarrow tH^-$ & $gg \rightarrow t\bar{b}H^-$)
- (EW processes : $gg \rightarrow W^\pm H^\mp$, $b\bar{b} \rightarrow W^\pm H^\mp$ & $q\bar{q}' \rightarrow W^{\pm*} \rightarrow \phi H^\pm$)
- 3. Resonant charged Higgs production : $c\bar{s} \rightarrow H^+$, $c\bar{b} \rightarrow H^+$
- 4. Charged Higgs pair production through $q\bar{q}$ annihilation or gluon fusion.
- **5. Same-sign charged Higgs pair production :**

$$pp \rightarrow W^{\pm*}W^{\pm*}jj \rightarrow H^\pm H^\pm jj$$

Physics Letters B

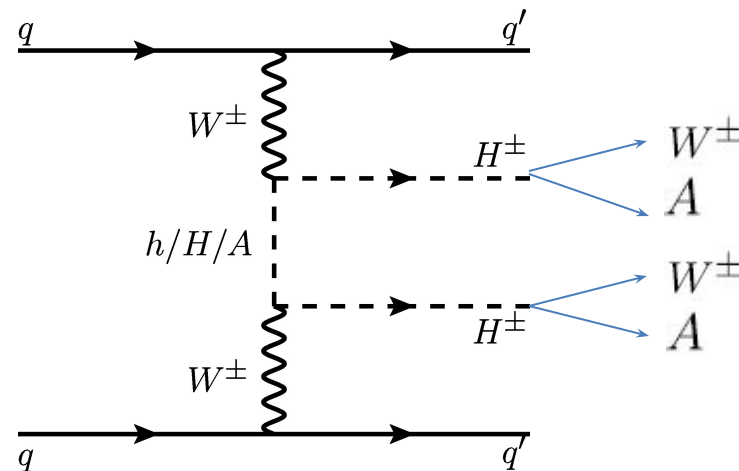
Volume 797, 10 October 2019, 134854

Masashi Aiko, Shinya Kanemura, Kentarou Mawatari (Osaka U.)

arXiv:1906.09101

Same-sign charged Higgs pair production

- 1. The full process : $pp \rightarrow W^{\pm*}W^{\pm*} \rightarrow jjH^{\pm}H^{\pm} \rightarrow jj(W^{\pm}A^0)(W^{\pm}A^0)$
- 2. The production cross section scales as the square of the mass difference $\Delta m = (m_{H^0} - m_{A^0})$ in the alignment limit $(\cos(\beta - \alpha) = 0)$
- 3. We focus on light pseudoscalar and large mass difference with
- $m_{A^0} = 30 - 100 \text{ GeV}$, $\Delta m \equiv m_{H^0} - m_{A^0} = 200 - 250 \text{ GeV}$
- in Type-I and III 2HDM's.



Contents

- 1. Motivation
- **2. Brief review of 2HDM's**
- 3. Constraints on 2HDM's
- 4. Same-sign charged Higgs pair production
- 5. Conclusions

Brief review of 2HDMs

In the two-Higgs-Doublet Model (2HDM), two Higgs doublet fields $\Phi_{1,2}$ with hypercharge $Y_{\Phi_{1,2}} = 1/2$ are introduced. The most general renormalizable scalar potential, which respects the $SU_L(2) \otimes U_Y(1)$ gauge symmetry, has the following form:

$$\begin{aligned} V(\Phi_1, \Phi_2) = & m_{11}^2 \Phi_1^\dagger \Phi_1 + m_{22}^2 \Phi_2^\dagger \Phi_2 + m_{12}^2 (\Phi_1^\dagger \Phi_2 + \Phi_2^\dagger \Phi_1) + \frac{\lambda_1}{2} (\Phi_1^\dagger \Phi_1)^2 + \frac{\lambda_2}{2} (\Phi_2^\dagger \Phi_2)^2 \\ & + \lambda_3 \Phi_1^\dagger \Phi_1 \Phi_2^\dagger \Phi_2 + \lambda_4 \Phi_1^\dagger \Phi_2 \Phi_2^\dagger \Phi_1 + \frac{\lambda_5}{2} \left[(\Phi_1^\dagger \Phi_2)^2 + (\Phi_2^\dagger \Phi_1)^2 \right] \end{aligned} \quad (2)$$

where m_{11}^2 , m_{22}^2 and $\lambda_{1,2,3,4}$ are real, while m_{12}^2 and λ_5 could be complex for CP violation purpose.

Brief review of 2HDMs

Assuming that both Φ_1 and Φ_2 acquire a vacuum expectation value (VEV) $v_{1,2}$ that can induce electroweak symmetry breaking, the two complex scalar $SU_L(2)$ doublets can be decomposed according to

$$\Phi_i = \begin{pmatrix} \phi_i^+ \\ (v_i + \rho_i + i\eta_i)/\sqrt{2} \end{pmatrix}, \quad i = 1, 2. \quad (3)$$

The mass eigenstates for the Higgs sector are obtained by orthogonal transformations,

$$\begin{pmatrix} \phi_1^\pm \\ \phi_2^\pm \end{pmatrix} = R_\beta \begin{pmatrix} G^\pm \\ H^\pm \end{pmatrix}, \quad \begin{pmatrix} \rho_1 \\ \rho_2 \end{pmatrix} = R_\alpha \begin{pmatrix} H^0 \\ h^0 \end{pmatrix}, \quad \begin{pmatrix} \eta_1 \\ \eta_2 \end{pmatrix} = R_\beta \begin{pmatrix} G^0 \\ A^0 \end{pmatrix},$$

with the generic form ($\theta = \alpha, \beta$)

$$R_\theta = \begin{pmatrix} \cos \theta & -\sin \theta \\ \sin \theta & \cos \theta \end{pmatrix}. \quad \tan \beta \equiv v_2/v_1$$

Brief review of 2HDMs

We are then left with seven independent parameters which can be taken as:

the four physical masses m_h, m_H, m_A and $m_{H\pm}$, CP-even mixing angle α , $\tan \beta$ and m_{12}^2 .

In order to avoid Flavor-Changing Neutral Current (FCNC), a discrete symmetry Z_2 (where for example $\Phi_1 \rightarrow \Phi_1$ and $\Phi_2 \rightarrow -\Phi_2$) is imposed

The most general Yukawa interaction can be written as follows

$$-\mathcal{L}_{\text{Yukawa}}^{\text{2HDM}} = \overline{Q}_L Y_u \tilde{\Phi}_2 u_R + \overline{Q}_L Y_d \Phi_d d_R + \overline{L}_L Y_\ell \Phi_\ell \ell_R + \text{h.c.},$$

where $\Phi_{d,l}$ ($d, l = 1, 2$) represent Φ_1 or Φ_2 , Y_f ($f = u, d$ or ℓ) stand for 3×3 Yukawa matrices and $\tilde{\Phi}_2 = i\sigma_2 \Phi_2^*$.

Brief review of 2HDMs

$$\begin{aligned}
 -\mathcal{L}_{\text{Yukawa}}^{2\text{HDM}} = & \sum_{f=u,d,\ell} \frac{m_f}{v} \left(\xi_f^{h^0} \bar{f} f h^0 + \xi_f^{H^0} \bar{f} f H^0 - i \xi_f^{A^0} \bar{f} \gamma_5 f A^0 \right) \\
 & + \left\{ \frac{\sqrt{2} V_{ud}}{v} \bar{u} \left(m_u \xi_u^{A^0} P_L + m_d \xi_d^{A^0} P_R \right) d H^+ + \frac{\sqrt{2} m_\ell \xi_\ell^{A^0}}{v} \bar{\nu}_L \ell_R H^+ + \text{h.c} \right\}
 \end{aligned}$$

Model	u_R^i	d_R^i	e_R^i
Type I	Φ_2	Φ_2	Φ_2
Type II	Φ_2	Φ_1	Φ_1
Lepton-specific	Φ_2	Φ_2	Φ_1
Flipped	Φ_2	Φ_1	Φ_2

type	$\xi_u^{A^0}$	$\xi_d^{A^0}$	$\xi_l^{A^0}$
I	$\cot \beta$	$-\cot \beta$	$-\cot \beta$
II	$\cot \beta$	$\tan \beta$	$\tan \beta$
III	$\cot \beta$	$-\cot \beta$	$\tan \beta$
IV	$\cot \beta$	$\tan \beta$	$-\cot \beta$

Contents

- 1. Motivation
- 2. Brief review of 2HDM's
- **3. Constraints on 2HDM's**
- 4. Same-sign charged Higgs pair production
- 5. Conclusions

Constraints on 2HDM's

Theoretical constraints :

- (1) All set of tree-level perturbative unitarity conditions
- (2) All λ_i 's remain perturbative
- (3) The potential remains bounded from below,

$$\lambda_1 > 0, \lambda_2 > 2, \sqrt{\lambda_1 \lambda_2} + \lambda_3 + \min(0, \lambda_4 + \lambda_5, \lambda_4 - \lambda_5)$$

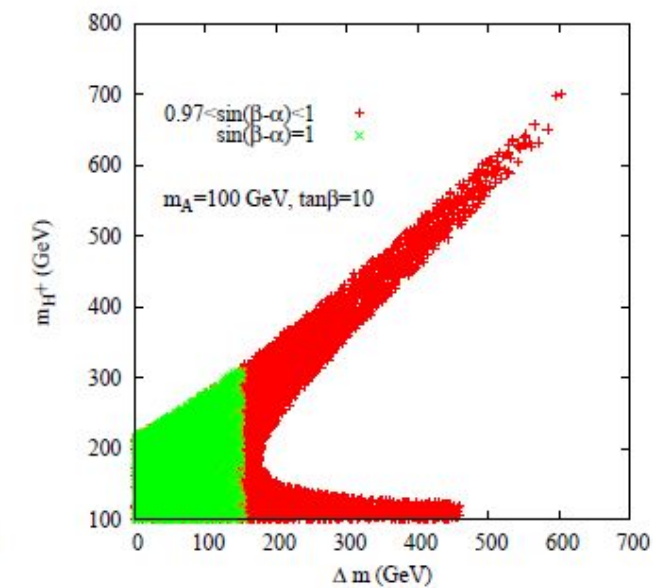
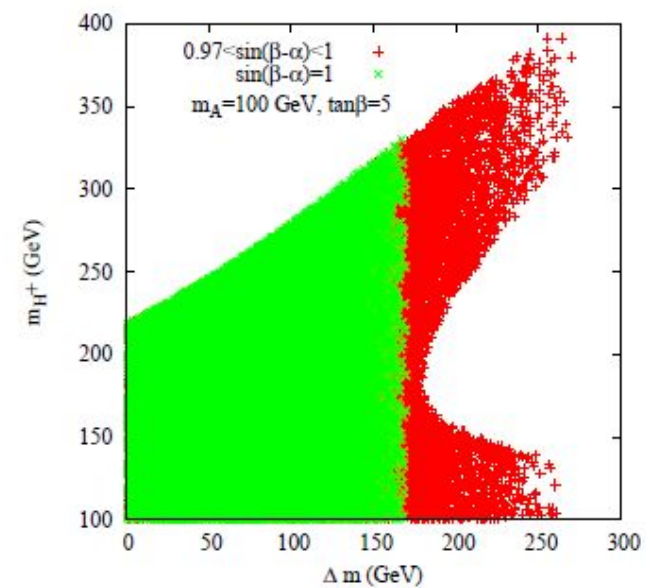
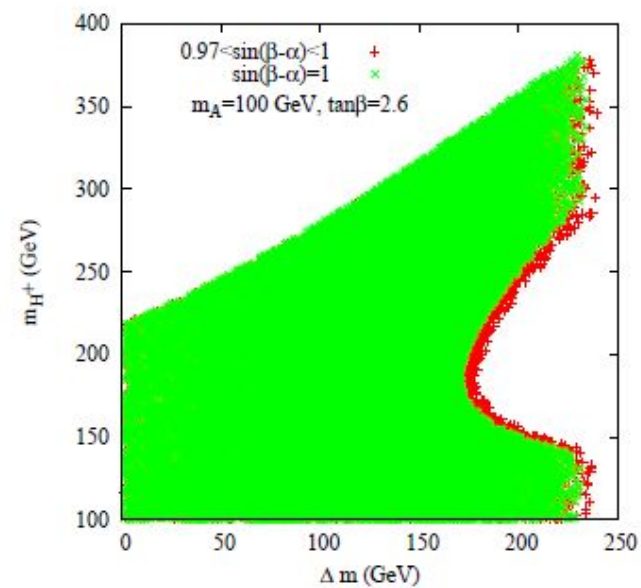
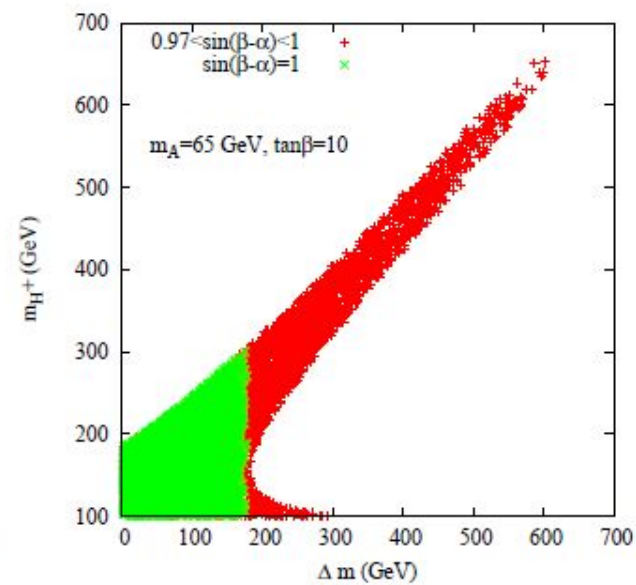
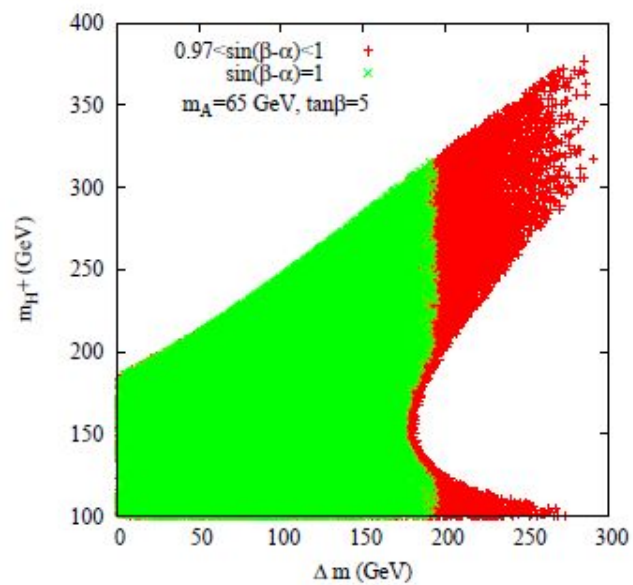
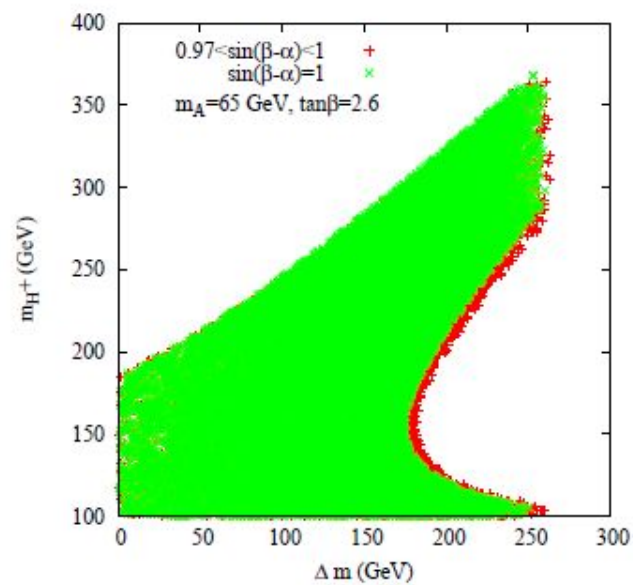
Experimental constraints from indirect searches :

- (1) Electro-Weak Precision Observable (EWPOs)
- (2) Flavor physics

Electro-Weak Precision Observable (EWPOs)

- The EWPOs can be represented by a set of oblique parameters S , T and U .
- We emphasize that the T parameter, which is related to the amount of isospin violation, is sensitive to the mass splitting among H^\pm , H^0 , and A^0 .
- From 2018 PDG review with fixed $U=0$, the best fit of S , T parameters can be represented as

$$S = 0.02 \pm 0.07 \quad T = 0.06 \pm 0.06$$



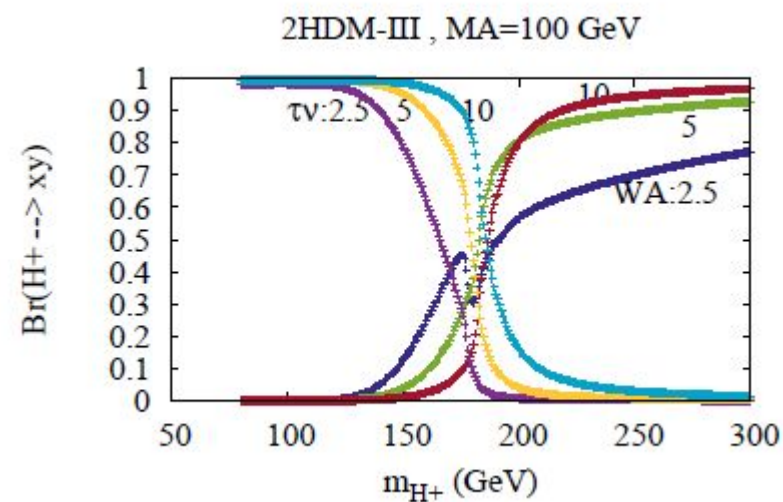
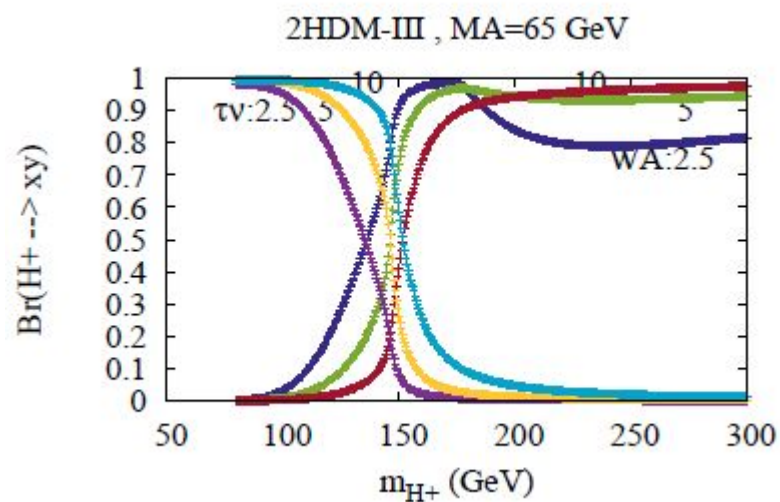
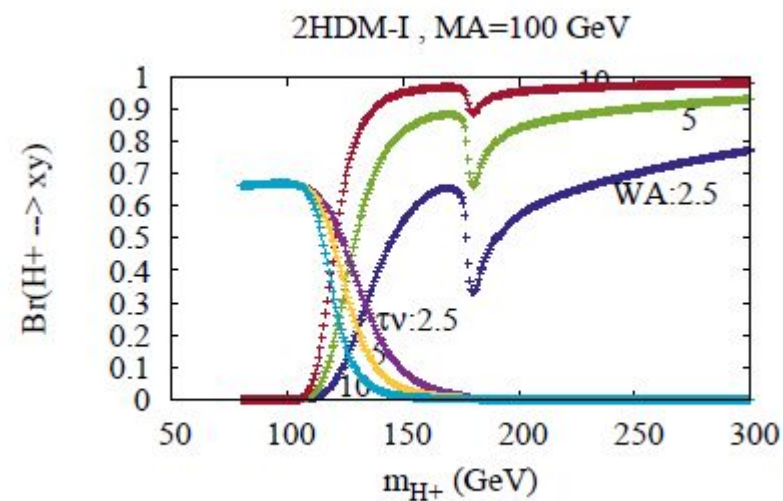
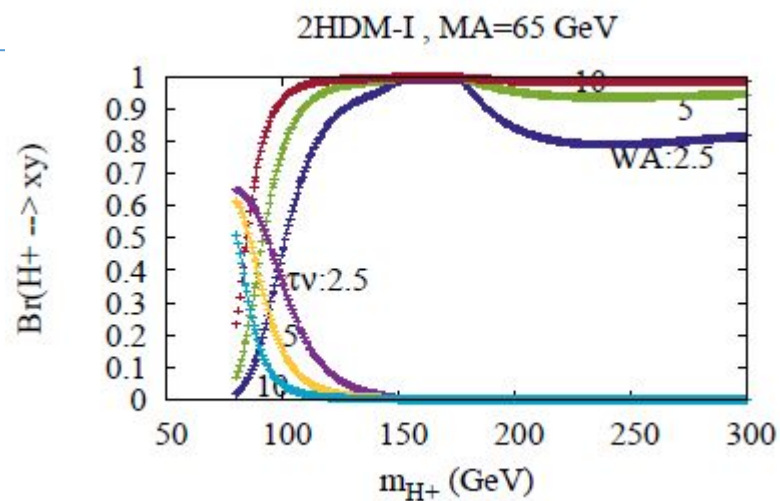
B physics constraints

The most severe constraints in flavor physics are due to the measurements of $B(B \rightarrow X_s \gamma)$, $B(B_{d,s} \rightarrow \mu^+ \mu^-)$ and Δm_s of B mesons. For $B(B \rightarrow X_s \gamma)$, according to the latest analysis by [30], we have:

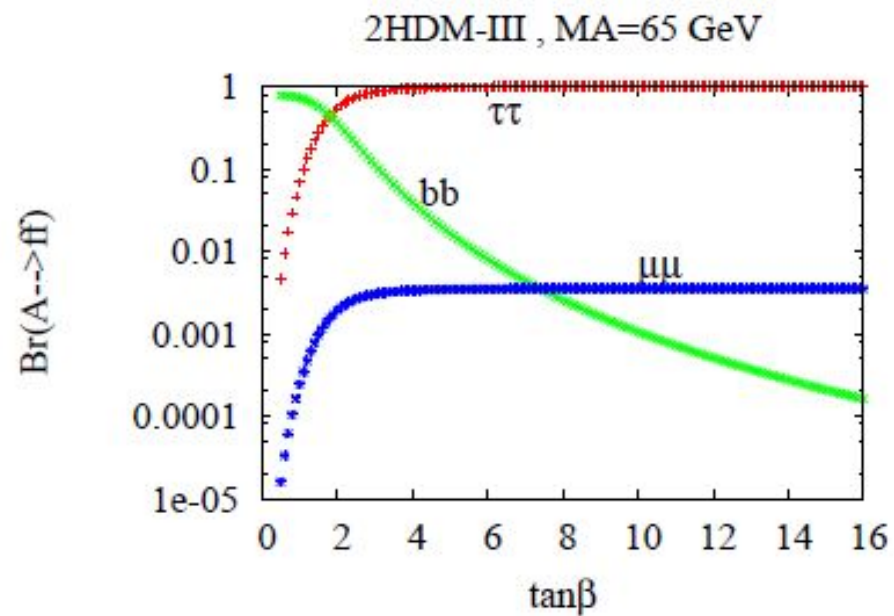
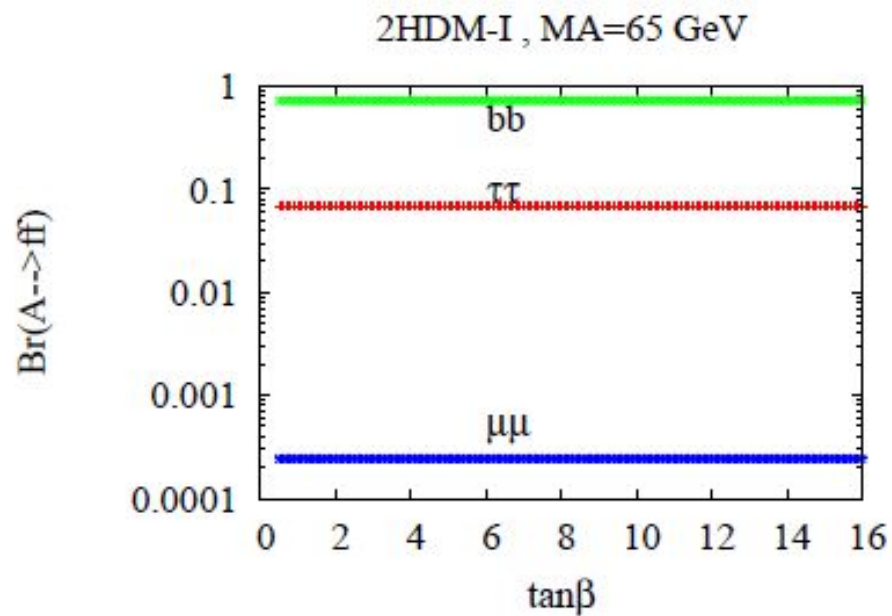
- In 2HDM type-II and IV, the $b \rightarrow s \gamma$ constraint forces the charged Higgs mass to be heavier than 580 GeV [30, 31] for any value of $\tan \beta \geq 1$.
- In 2HDM-I and III, charged Higgs with mass as low as $\sim 100 - 200$ GeV [30, 32] is still allowed as long as $\tan \beta \geq 2$.

For other B-physics observables we refer to the recent analysis [33], in which they also included Δm_s and $B_{d,s} \rightarrow \mu^+ \mu^-$. For a light charged Higgs boson, $100 < m_{H^\pm} < 200$ GeV, of interest in this study, one can conclude from [33] that $\tan \beta \geq 3$ is allowed for 2HDM type I and III.

H^\pm and A^0 branching ratios and Direct searches



H^\pm and A^0 branching ratios and Direct searches

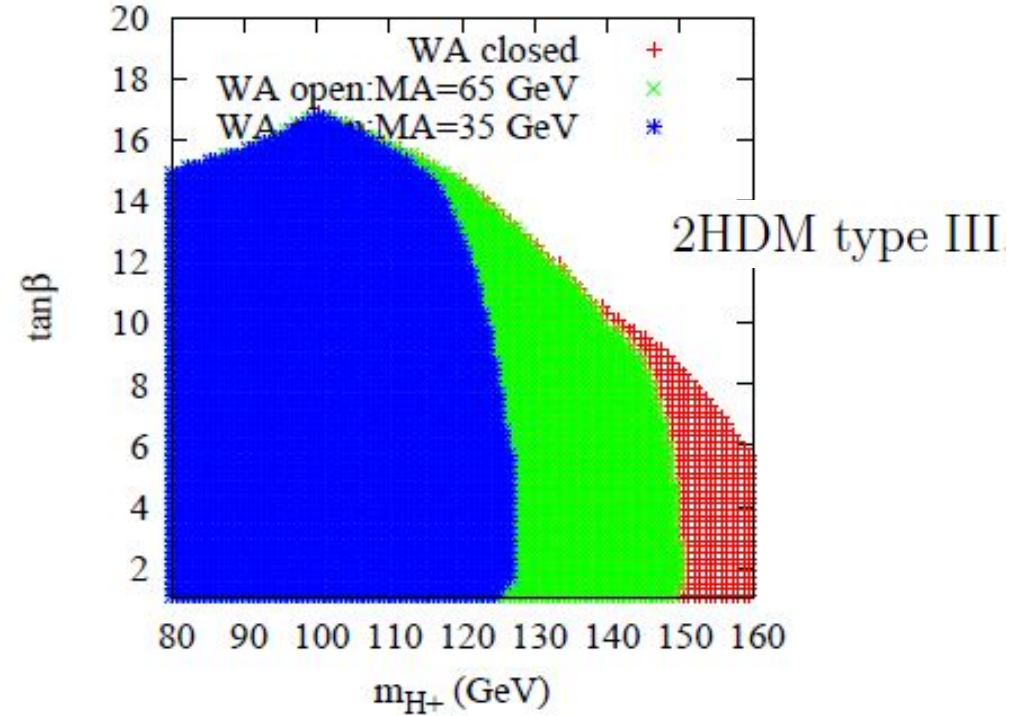
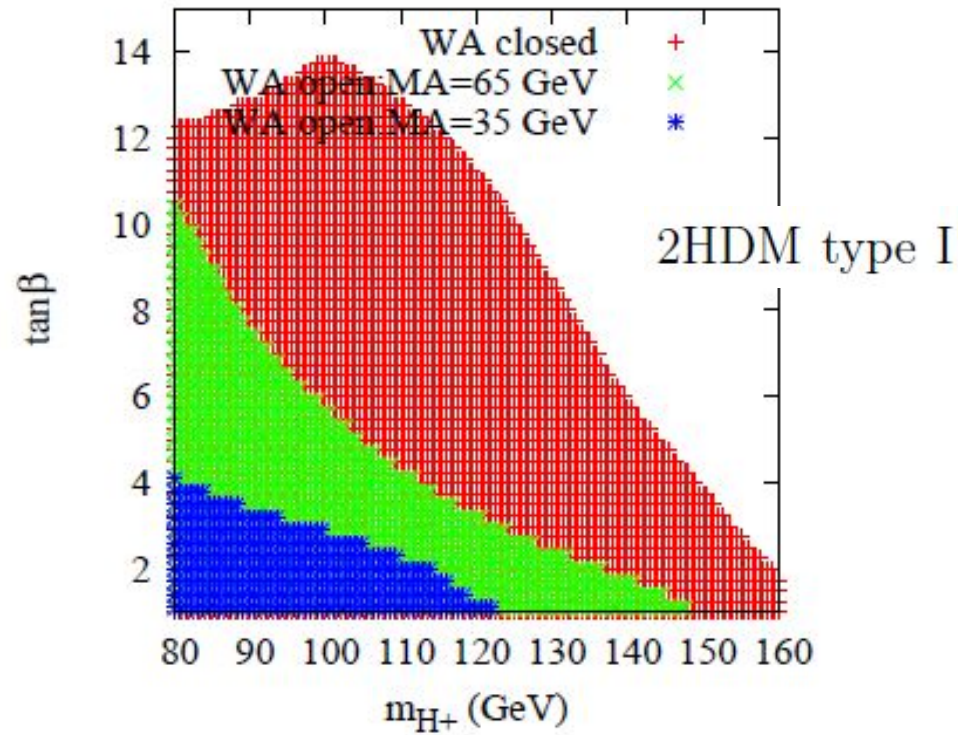


LHC Constraint from $t \rightarrow bH^+ \rightarrow b\tau\nu_\tau$

CMS Collaboration JHEP 07 (2019) 142

arXiv:1903.04560

Search for charged Higgs bosons in the $H^\pm \rightarrow \tau^\pm \nu_\tau$ decay channel in proton-proton collisions at $\sqrt{s} = 13$ TeV



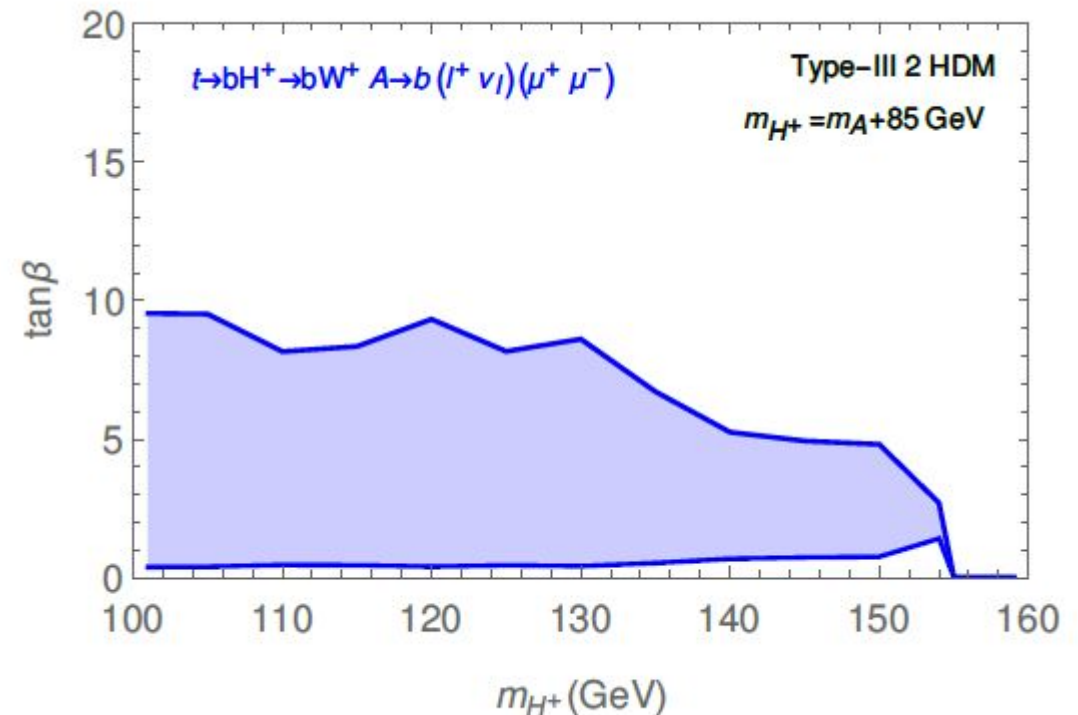
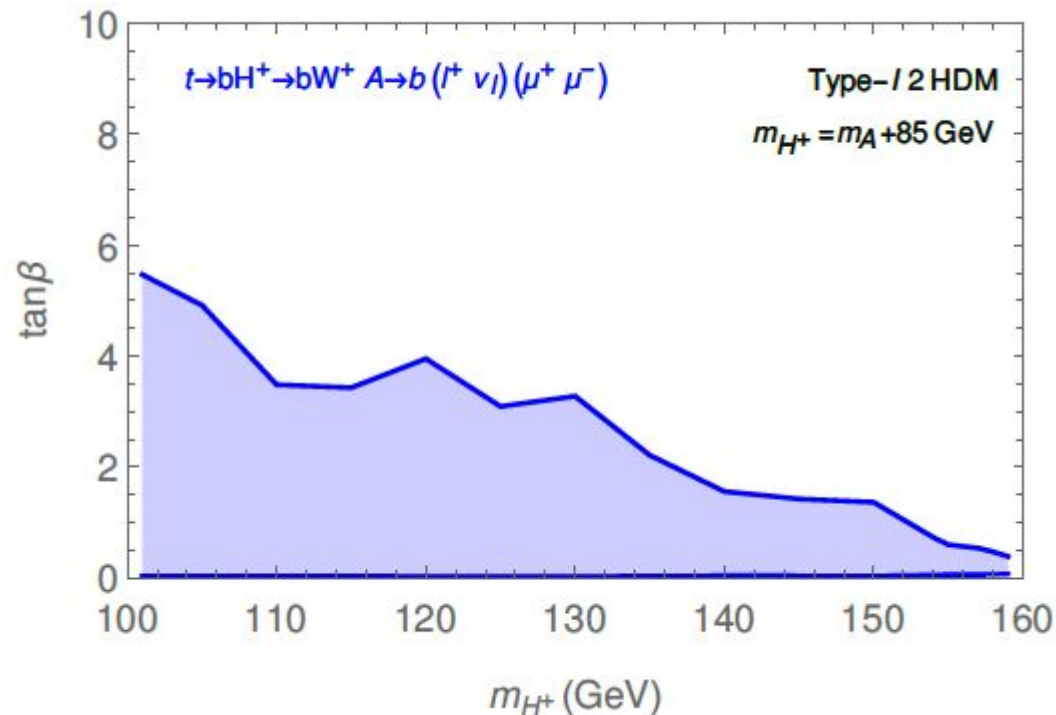
LHC Constraint from $t \rightarrow bH^+ \rightarrow bA^0W^+ \rightarrow bW^+\mu^+\mu^-$

CMS Collaboration

Phys. Rev. Lett. 123, 131802 (2019)

arXiv:1905.07453

Search for a light charged Higgs boson decaying to a W boson and a CP-odd Higgs boson in final states with $e\mu\mu$ or $\mu\mu\mu$ in proton-proton collisions at $\sqrt{s} = 13$ TeV



Contents

- 1. Motivation
- 2. Brief review of 2HDM's
- 3. Constraints on 2HDM's
- **4. Same-sign charged Higgs pair production**
- 5. Conclusions

The behavior of $pp \rightarrow H^\pm H^\pm j_F j_F$ process

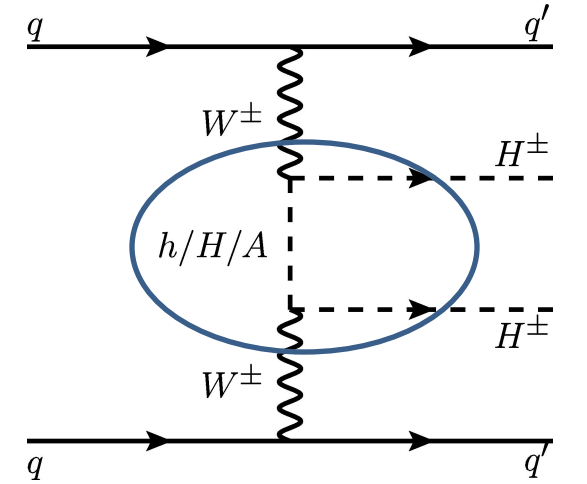
The relation between the mass splitting Δm and same-sign charged Higgs pair production can be understood in the $2 \rightarrow 2$ subprocess $W^+ W^+ \rightarrow H^+ H^+$ at amplitude level. This subprocess is induced by three t-channel diagrams with h^0 , H^0 and A^0 exchange. In the alignment limit, $\cos(\beta - \alpha) = 0$, which is favored by the current Higgs data, the scattering amplitude for

$$W^+(p_1) W^+(p_2) \rightarrow H^+(q_1) H^+(q_2)$$

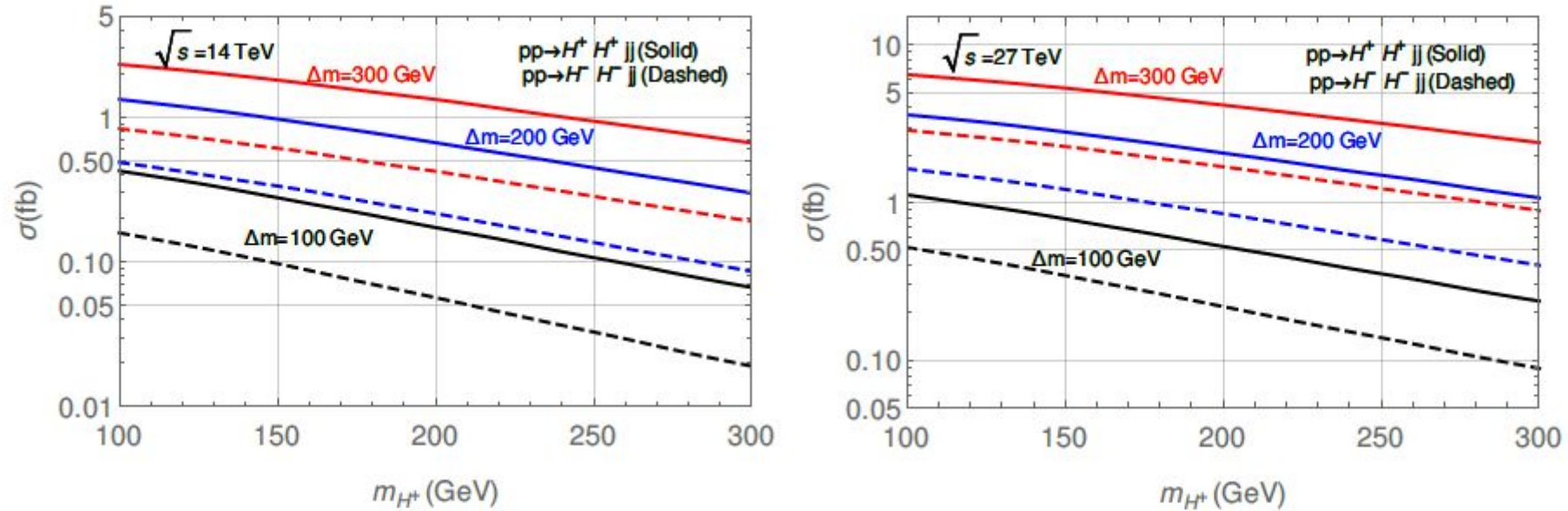
is only mediated by H^0 and A^0 and is given by

$$\begin{aligned} i\mathcal{M}^{H^0+A^0} &= ig^2 q_1 \cdot \epsilon(p_1) q_2 \cdot \epsilon(p_2) \left[\frac{1}{t-m_{A^0}^2} - \frac{1}{t-m_{H^0}^2} \right] + (q_1 \leftrightarrow q_2, t \leftrightarrow u) \\ &\propto \Delta m \times \frac{m_{H^0} + m_{A^0}}{(t-m_{H^0}^2)(t-m_{A^0}^2)} q_1 \cdot \epsilon(p_1) q_2 \cdot \epsilon(p_2) + (q_1 \leftrightarrow q_2, t \leftrightarrow u) \end{aligned} \quad (9)$$

where $t = (p_1 - q_1)^2$ and $u = (p_1 - q_2)^2$, and $\epsilon(p_{1,2})$ are the polarization 4-vector of the incoming W^+ bosons. As it can be seen, the above amplitude is proportional to Δm .



The behavior of $pp \rightarrow H^\pm H^\pm j_F j_F$ process



alignment limit ($\cos(\beta - \alpha) = 0$)

FIG. 6. The production cross sections of $pp \rightarrow H^+ H^+ j_F j_F$ (solid line) and $pp \rightarrow H^- H^- j_F j_F$ (dashed line) versus m_{H^\pm} at $\sqrt{s} = 14$ TeV (left panel) and $\sqrt{s} = 27$ TeV (right panel), for $\Delta m = 100$ GeV (black), 200 GeV (blue), and 300 GeV (red). Notice the VBF cut $\eta_{j_1} \times \eta_{j_2} < 0$ and $|\Delta\eta_{jj}| > 2.5$ for the minimum rapidity difference between the forward jet pair are applied.

Signal-background analysis for Type-I 2HDM

- The signal process

$$pp \rightarrow W^{\pm*}W^{\pm*}j_Fj_F \rightarrow H^{\pm}H^{\pm}j_Fj_F \rightarrow (W^{\pm}A^0)(W^{\pm}A^0)j_Fj_F \rightarrow l^{\pm}\nu(b\bar{b})l^{\pm}\nu(b\bar{b})j_Fj_F$$

- The main SM backgrounds

$$pp \rightarrow t\bar{t}t\bar{t} \rightarrow (bW^+)(\bar{b}W^-)(bW^+)(\bar{b}W^-) \rightarrow l^{\pm}l^{\pm}4b4j,$$

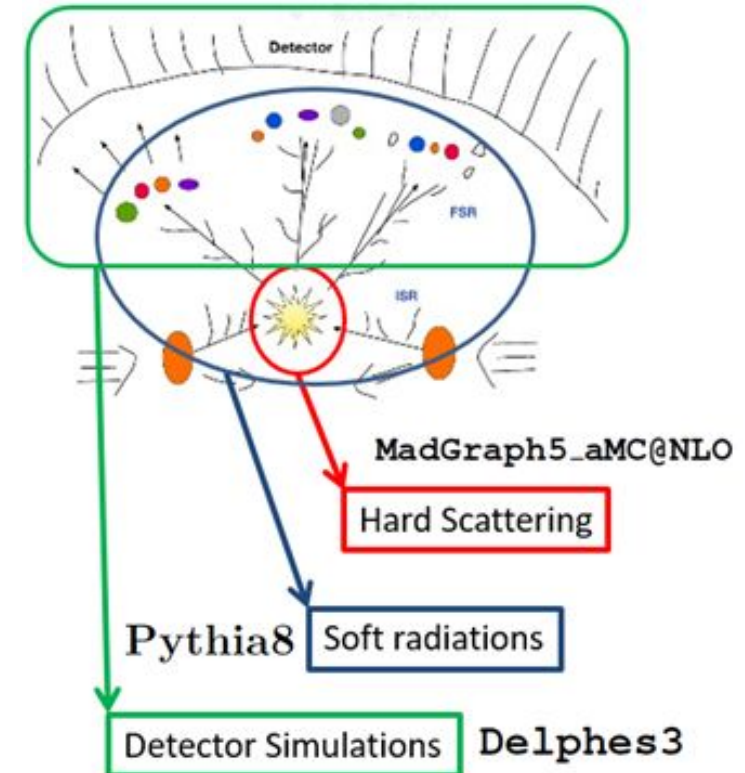
$$pp \rightarrow t\bar{t}t\bar{b}l^+l^- \rightarrow (bW^+)\bar{b}(\bar{b}W^-)bl^+l^- \rightarrow l^{\pm}l^+l^-4b2j,$$

$$pp \rightarrow t\bar{t}t\bar{b} \rightarrow (bW^+)(\bar{b}W^-)(bW^+)\bar{b} \rightarrow l^+l^+4b2j$$

$$\text{or } pp \rightarrow t\bar{t}t\bar{b} \rightarrow (bW^+)(\bar{b}W^-)(\bar{b}W^-)b \rightarrow l^-l^-4b2j,$$

$$pp \rightarrow t\bar{t}b\bar{b}jj \rightarrow (bW^+)(bW^+)\bar{b}\bar{b}jj \rightarrow l^+l^+4b2j$$

$$\text{or } pp \rightarrow t\bar{t}b\bar{b}jj \rightarrow (\bar{b}W^-)(\bar{b}W^-)bbjj \rightarrow l^-l^-4b2j.$$

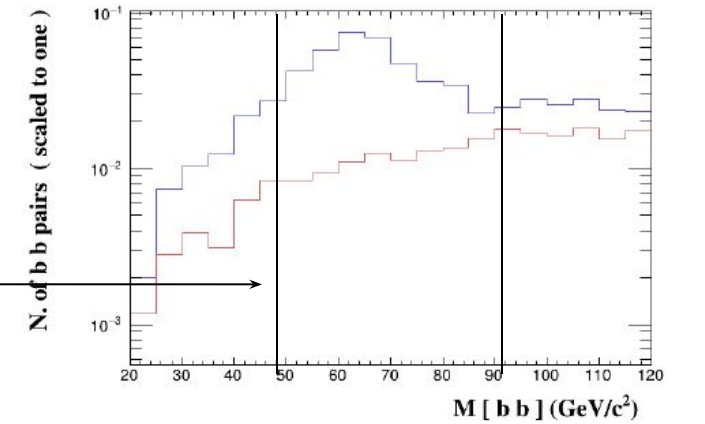
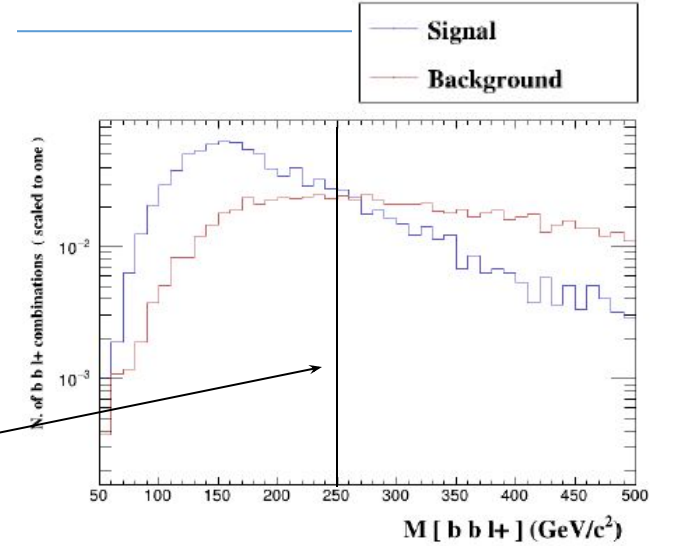


Signal-background analysis for Type-I 2HDM

TABLE IV. Cut flow table for the Type-I 2HDM signal $pp \rightarrow H^\pm H^\pm j_F j_F$ with $m_{H^\pm} = 205$ GeV, $m_{A^0} = 65$ GeV, $\Delta m = 200$ GeV, $\tan \beta = 5$ and $\sin(\beta - \alpha) = 0.97$, and various backgrounds at $\sqrt{s} = 14$ TeV.

MadAnalysis5

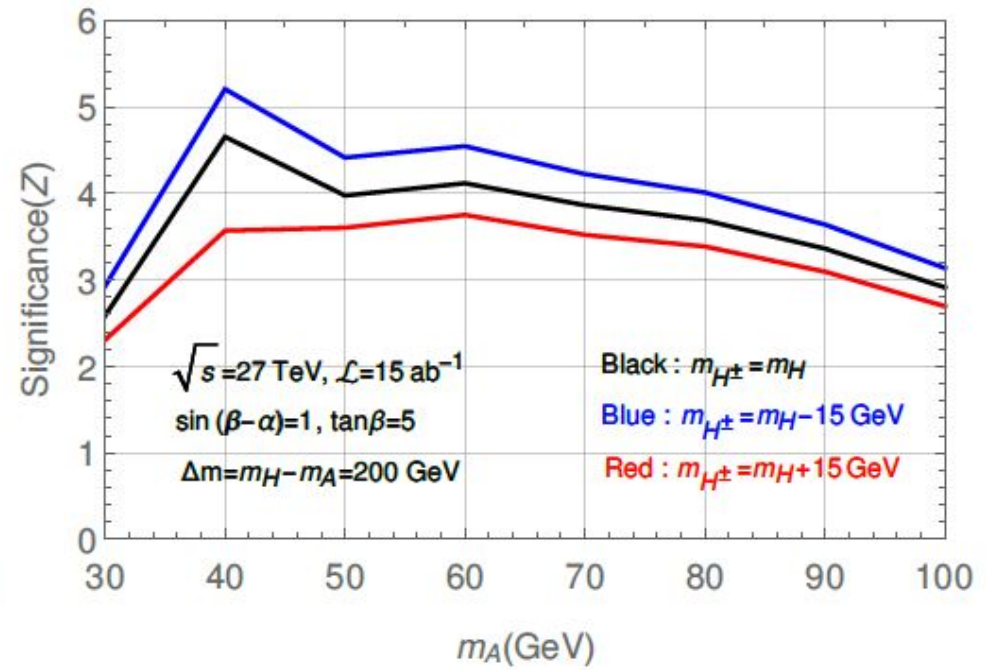
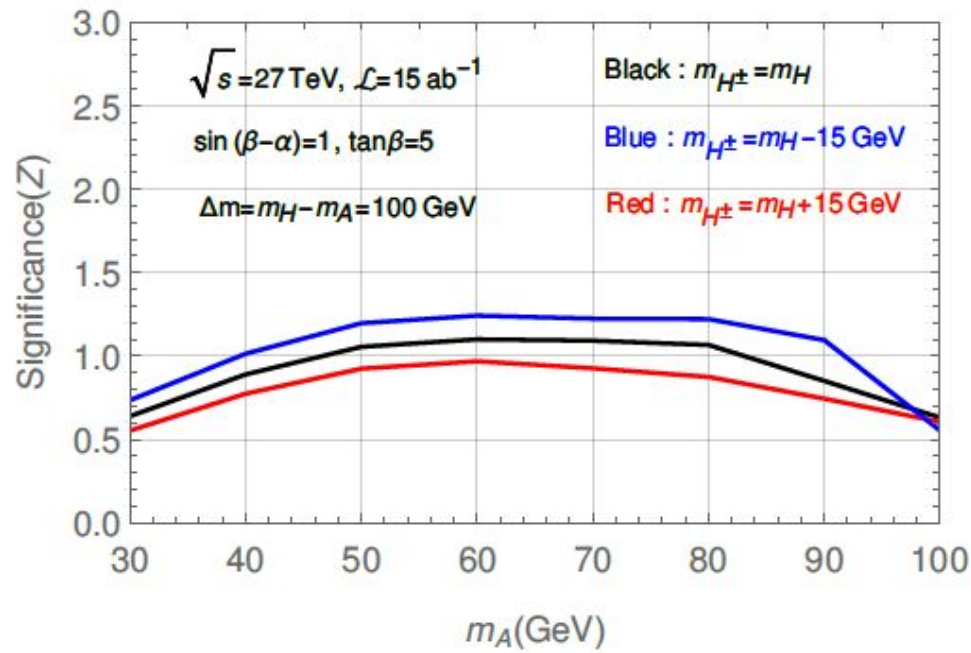
Cross section (fb)	signal	$t\bar{t}t\bar{t}$	$t\bar{t}b\bar{b}l^+l^-$	$3t1b$	$2t2b2j$
Preselection	2.07×10^{-2}	4.94×10^{-2}	1.08×10^{-2}	7.74×10^{-5}	8.29×10^{-5}
$N(b, l^\pm) \geq 3, 2,$					
$P_T^{b, l^\pm} > 20\text{GeV}, \eta^{b, l} < 2.5$	1.76×10^{-3}	6.17×10^{-3}	9.56×10^{-4}	9.57×10^{-6}	9.81×10^{-6}
$N(j) \geq 2,$					
$P_T^j > 30\text{GeV}, M_{jj} > 500\text{GeV}$	1.46×10^{-3}	5.15×10^{-3}	4.18×10^{-4}	2.88×10^{-6}	4.05×10^{-6}
m_{H^\pm} Cuts					
$M_{bbl^\pm} < 250\text{GeV}$	1.41×10^{-3}	3.50×10^{-3}	2.71×10^{-4}	1.85×10^{-6}	2.62×10^{-6}
m_A Cuts					
$50 < M_{bb} < 90\text{GeV}$	1.30×10^{-3}	1.68×10^{-3}	1.61×10^{-4}	7.58×10^{-7}	1.14×10^{-6}



Signal-background analysis for Type-I 2HDM

TABLE V. Cut flow table for the Type-I 2HDM signal $pp \rightarrow H^\pm H^\pm j_F j_F$ with $m_{H^\pm} = 205$ GeV, $m_{A^0} = 65$ GeV, $\Delta m = 200$ GeV, $\tan \beta = 5$ and $\sin(\beta - \alpha) = 0.97$, and various backgrounds at $\sqrt{s} = 27$ TeV. MadAnalysis5

Cross section (fb)	signal	$t\bar{t}\bar{t}$	$t\bar{t}b\bar{b}l^+l^-$	$3t1b$	$2t2b2j$
Preselection	6.88×10^{-2}	5.67×10^{-1}	5.60×10^{-2}	2.40×10^{-4}	6.76×10^{-4}
$N(b, l^\pm) \geq 3, 2,$					
$P_T^{b, l^\pm} > 20\text{GeV}, \eta^{b, l} < 2.5$	5.15×10^{-3}	5.67×10^{-2}	4.43×10^{-3}	2.44×10^{-5}	6.42×10^{-5}
$N(j) \geq 2,$					
$P_T^j > 30\text{GeV}, M_{jj} > 500\text{GeV}$	4.54×10^{-3}	5.22×10^{-2}	2.49×10^{-3}	9.67×10^{-6}	3.27×10^{-5}
m_{H^\pm} Cuts					
$M_{bbl^\pm} < 200\text{GeV}$	4.10×10^{-3}	2.28×10^{-2}	1.08×10^{-3}	4.29×10^{-6}	1.45×10^{-5}
m_A Cuts					
$50 < M_{bb} < 80\text{GeV}$	3.76×10^{-3}	1.12×10^{-2}	6.09×10^{-4}	1.91×10^{-6}	7.15×10^{-6}

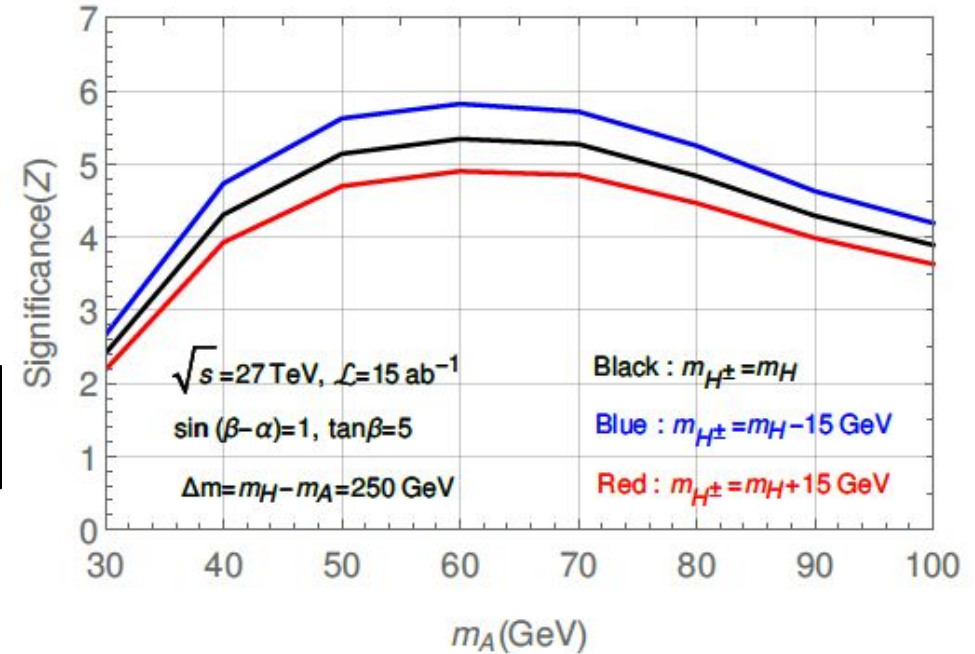


$$M_{bbl^\pm} \leq M_{H^\pm} - 5\text{ GeV}.$$

$$|M_{bb} - m_A| \leq 15\text{ GeV}.$$

The significance Z

$$Z = \sqrt{2} \cdot [((s+b) \cdot \ln(1+s/b) - s)]$$



Signal-background analysis for Type-III 2HDM

- The signal process

$$pp \rightarrow W^{\pm*} W^{\pm*} j_F j_F \rightarrow H^{\pm} H^{\pm} j_F j_F \rightarrow (W^{\pm} A^0)(W^{\pm} A^0) j_F j_F \rightarrow l^{\pm} \nu (\tau^+ \tau^-) l^{\pm} \nu (\tau^+ \tau^-) j_F j_F$$

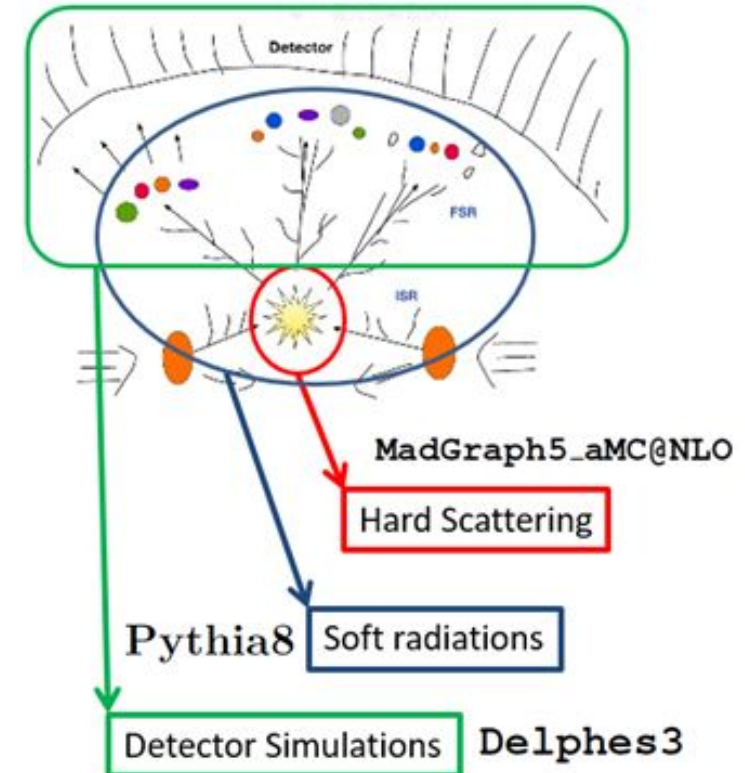
- The main SM backgrounds

$$pp \rightarrow t\bar{t} Z j j \rightarrow (b W^+) (\bar{b} W^-) (\tau^+ \tau^-) j j \rightarrow l^{\pm} 2b 3\tau 2j,$$

$$pp \rightarrow t\bar{t} W^{\pm} j j \rightarrow (b W^+) (\bar{b} W^-) (\tau^{\pm} \nu_{\tau}) j j \rightarrow l^{\pm} 2b 2\tau 2j,$$

$$pp \rightarrow W^{\pm} W^{\mp} Z j j \rightarrow (l^{\pm} \nu_l) (\tau^{\mp} \nu_{\tau}) (\tau^+ \tau^-) j j \rightarrow l^{\pm} 3\tau 2j,$$

$$pp \rightarrow W^{\pm} Z Z j j \rightarrow (l^{\pm} \nu_l) (\tau^+ \tau^-) (\tau^+ \tau^-) j j \rightarrow l^{\pm} 4\tau 2j$$

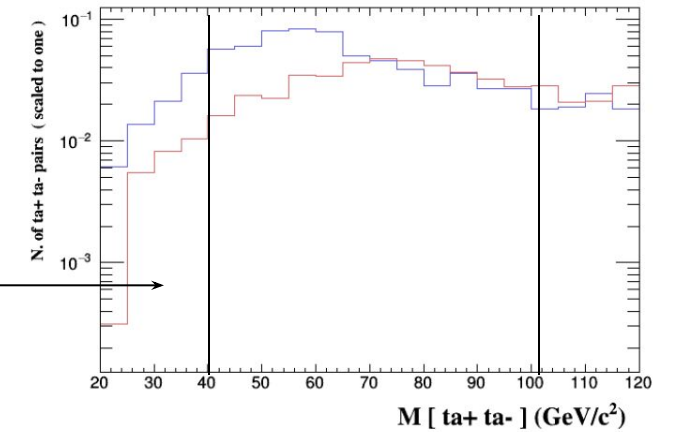
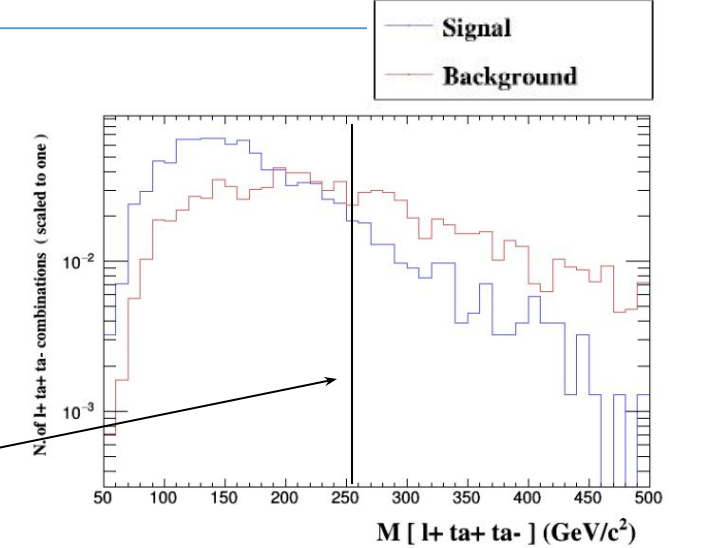


Signal-background analysis for Type-III 2HDM

TABLE VI. Cut flow table for the Type-III 2HDM signal $pp \rightarrow H^\pm H^\pm j_F j_F$ with $m_{H^\pm} = 205$ GeV, $m_{A^0} = 65$ GeV, $\Delta m = 200$ GeV, $\tan \beta = 5$ and $\sin(\beta - \alpha) = 0.97$, and various backgrounds at $\sqrt{s} = 14$ TeV.

MadAnalysis5

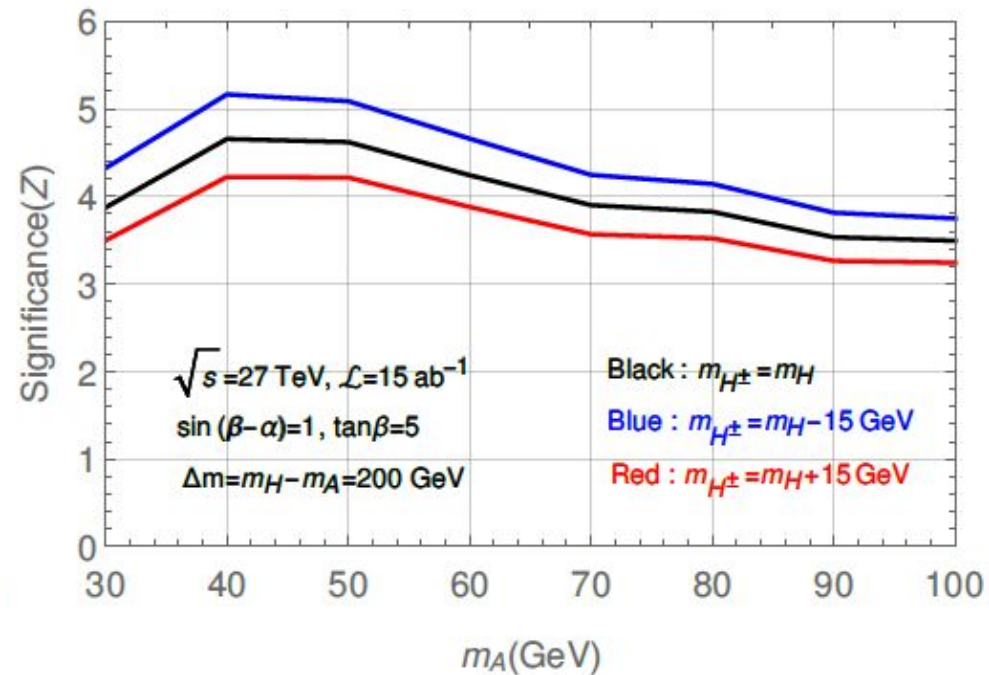
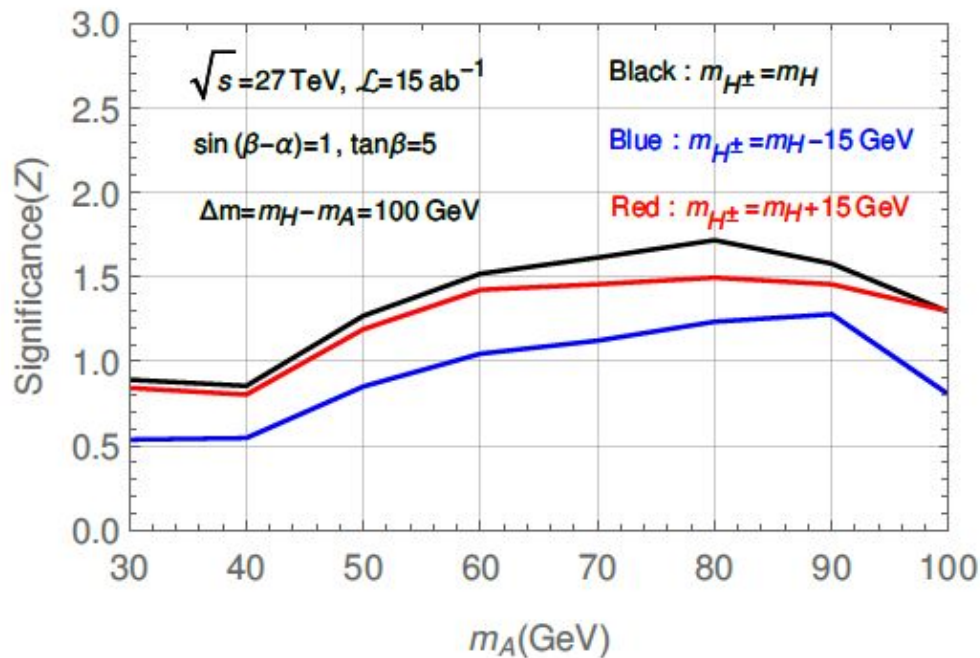
Cross section (fb)	signal	$t\bar{t}Zjj$	$t\bar{t}W^\pm jj$	$W^\pm W^\mp Zjj$	$W^\pm ZZjj$
Preselection	2.98×10^{-2}	3.60×10^{-1}	2.44×10^{-1}	3.28×10^{-2}	1.87×10^{-3}
$N(\tau, l^\pm) \geq 3, 2,$					
$P_T^{\tau, l^\pm} > 20\text{GeV}, \eta^{\tau, l} < 2.5$	1.23×10^{-3}	7.42×10^{-3}	1.07×10^{-3}	3.89×10^{-4}	9.61×10^{-5}
$N(j) \geq 2,$					
$P_T^j > 30\text{GeV}, M_{jj} > 500\text{GeV}$	9.81×10^{-4}	4.63×10^{-3}	6.19×10^{-4}	1.97×10^{-4}	5.08×10^{-5}
b-jet veto	9.15×10^{-4}	1.15×10^{-3}	2.03×10^{-4}	1.71×10^{-4}	4.32×10^{-5}
m_{H^\pm} Cut					
$M_{\tau+\tau-l^\pm} < 250\text{GeV}$	8.24×10^{-4}	7.52×10^{-4}	9.18×10^{-5}	1.15×10^{-4}	2.98×10^{-5}
m_{A^0} Cut					
$40 < M_{\tau+\tau^-} < 100\text{GeV}$	7.95×10^{-4}	6.28×10^{-4}	5.81×10^{-5}	1.04×10^{-4}	2.73×10^{-5}



Signal-background analysis for Type-III 2HDM

TABLE VII. Cut flow table for the Type-III 2HDM signal $pp \rightarrow H^\pm H^\pm j_F j_F$ with $m_{H^\pm} = 205$ GeV, $m_{A^0} = 65$ GeV, $\Delta m = 200$ GeV, $\tan \beta = 5$ and $\sin(\beta - \alpha) = 0.97$, and various backgrounds at $\sqrt{s} = 27$ TeV. MadAnalysis5

Cross section (fb)	signal	$t\bar{t}Zjj$	$t\bar{t}W^\pm jj$	$W^\pm W^\mp Zjj$	$W^\pm ZZjj$
Preselection	9.93×10^{-2}	2.51	1.49	1.51×10^{-1}	8.62×10^{-3}
$N(\tau, l^\pm) \geq 3, 2,$					
$P_T^{\tau, l^\pm} > 20\text{GeV}, \eta^{\tau, l} < 2.5$	4.27×10^{-3}	4.96×10^{-2}	6.14×10^{-3}	1.71×10^{-3}	4.04×10^{-4}
$N(j) \geq 2,$					
$P_T^j > 30\text{GeV}, M_{jj} > 500\text{GeV}$	3.71×10^{-3}	3.69×10^{-2}	4.50×10^{-3}	1.08×10^{-3}	2.67×10^{-4}
b-jet veto	3.40×10^{-3}	9.23×10^{-3}	1.41×10^{-3}	9.23×10^{-4}	2.19×10^{-4}
m_{H^\pm} Cut					
$M_{\tau^+\tau^-l^\pm} < 200\text{GeV}$	2.75×10^{-3}	4.04×10^{-3}	4.17×10^{-4}	3.94×10^{-4}	1.09×10^{-4}
m_{A^0} Cut					
$40 < M_{\tau^+\tau^-} < 70\text{GeV}$	2.35×10^{-3}	2.20×10^{-3}	1.96×10^{-4}	2.29×10^{-4}	6.63×10^{-5}

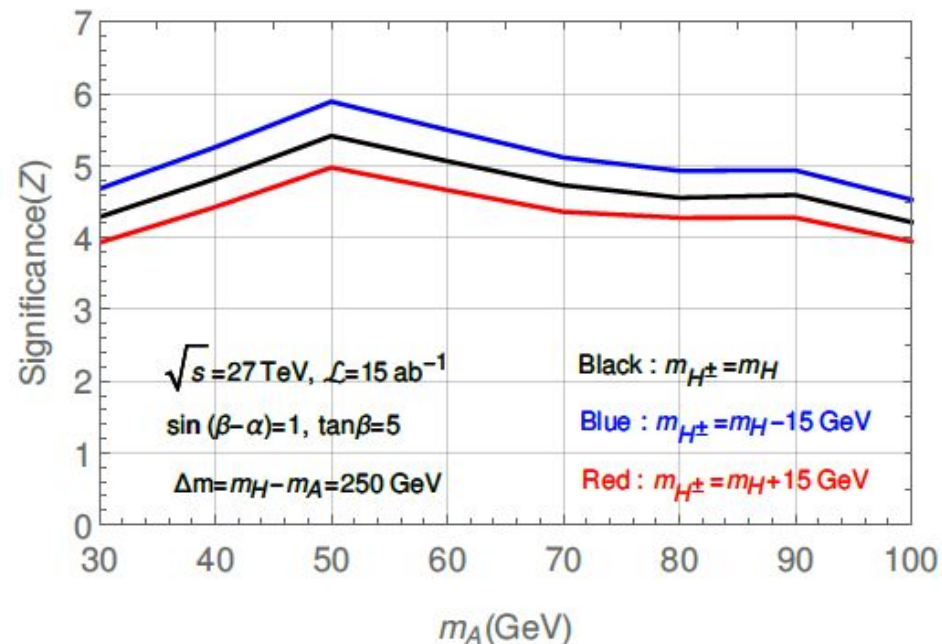


$$M_{\tau^+\tau^-l^\pm} \leq M_{H^\pm} - 5 \text{ GeV}.$$

$$m_{A^0} - 25 \text{ GeV} \leq M_{\tau^+\tau^-} \leq m_{A^0} + 5 \text{ GeV}.$$

The significance Z

$$Z = \sqrt{2} \cdot [((s + b) \cdot \ln(1 + s/b) - s)]$$



Contents

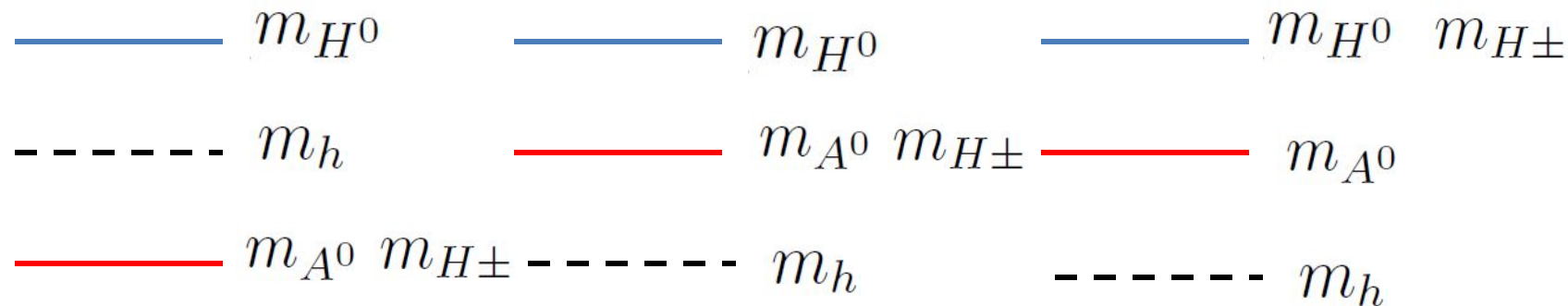
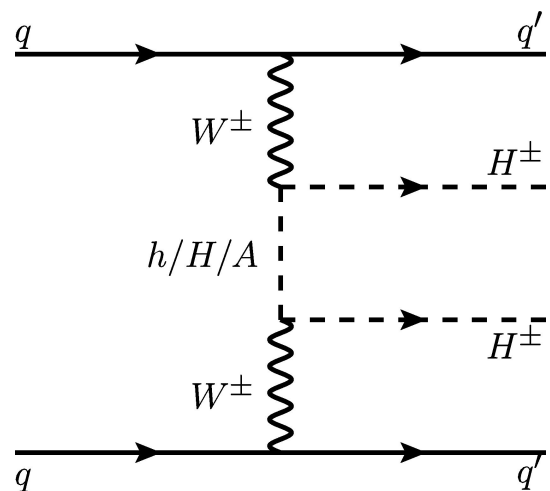
- 1. Motivation
- 2. Brief review of 2HDM's
- 3. Constraints on 2HDM's
- 4. Same-sign charged Higgs pair production
- **5. Conclusions**

Conclusions

- The 2HDM is one of the most popular extended Higgs sector with rich phenomenology.
- Exploring the whole mass spectrum in 2HDM can help us understand the mystery of EWSB.
- We have studied a novel process - **production of same-sign charged Higgs production**.

$$pp \rightarrow W^{\pm*} W^{\pm*} \rightarrow jj H^{\pm} H^{\pm} \rightarrow jj (W^{\pm} A^0) (W^{\pm} A^0)$$

- It allows one to probe the whole mass spectrum in the 2HDM for some specific relations.
- We have investigated same-sign charged Higgs-boson production via **vector-boson-fusion** at the HL-LHC and HE-LHC (27 TeV) in **Type I and III 2HDM's**.



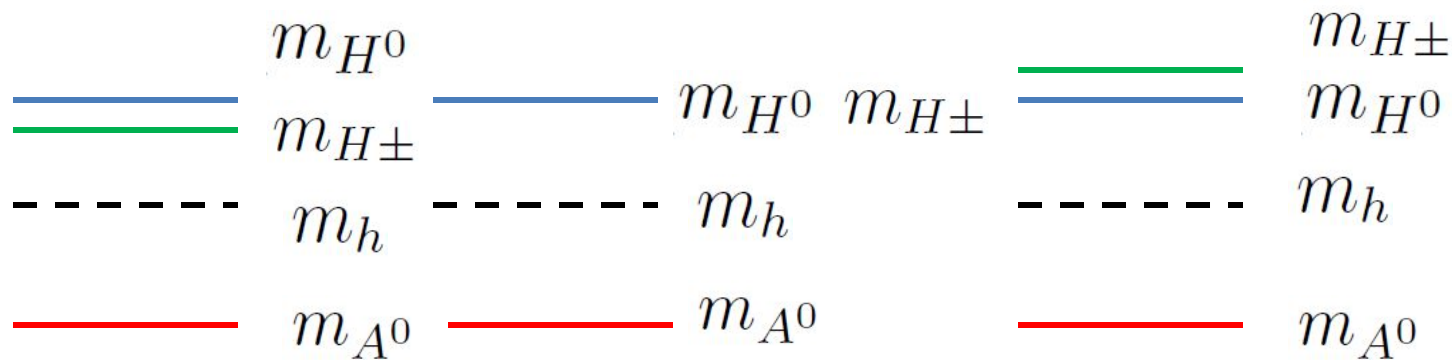
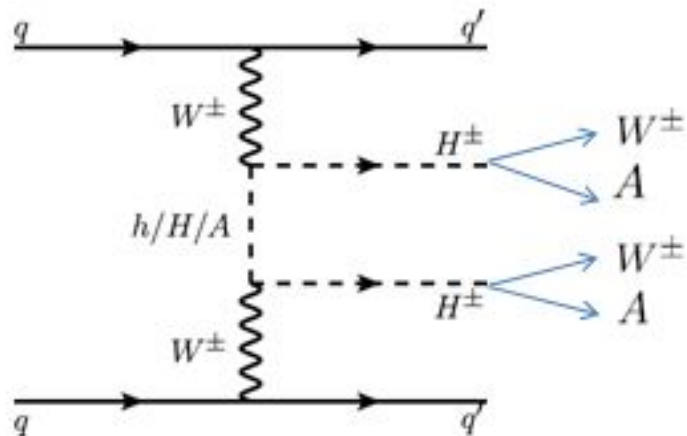
$$H^\pm \rightarrow \tau \nu \quad H^\pm \rightarrow tb$$

Masashi Aiko, Shinya Kanemura, Kentarou Mawatari (Osaka U.)

arXiv:1906.09101

Physics Letters B

Volume 797, 10 October 2019, 134854



$$A^0 \rightarrow b\bar{b} \quad A^0 \rightarrow \tau\tau$$

arXiv:1910.02571

Conclusions

In type I 2HDM, we used the decay channel $H^\pm H^\pm \rightarrow (W^\pm A^0)(W^\pm A^0) \rightarrow (l^\pm \nu b \bar{b}) (l^\pm \nu b \bar{b})$ together with a pair of forward jets to perform the signal-background analysis. At the end, we found about 4 signal events versus 5 background events at HL-LHC with luminosity of 3000 fb^{-1} for a typical benchmark point. At the HE-LHC, significance level of 2 – 5 can be achieved for $\Delta m = 200 - 250 \text{ GeV}$.

On the other hand, in type III 2HDM we used the decay channel $H^\pm H^\pm \rightarrow (W^\pm A^0)(W^\pm A^0) \rightarrow (l^\pm \nu \tau^+ \tau^-) (l^\pm \nu \tau^+ \tau^-)$ together with a pair of forward jets to perform the signal-background analysis. At the HL-LHC, we can achieve the signal-to-background ratio equal to 1, and the number of signal events is about 2 for a luminosity of 3000 fb^{-1} . Nevertheless, at the HE-LHC the significance can rise to the level of 3 – 6 for $\Delta m = 200 - 250 \text{ GeV}$.

Conclusions

In summary, the process in Eq. (1) can be an additional check of the mass relation between same-sign charged Higgs-boson production and Δm , especially, if the 2HDM mass spectrum has is as follow:

- one light (pseudo)scalar, say A^0 ,
- a large mass splitting between two neutral scalars, $\Delta m = (m_{H^0} - m_{A^0})$, and
- the charged Higgs mass is above the $W^\pm A^0$ threshold,

then this scenario can be either pinned down or ruled out in the near future.

Thank you
for your attention

경청해 주셔서 감사합니다

Back-up Slide

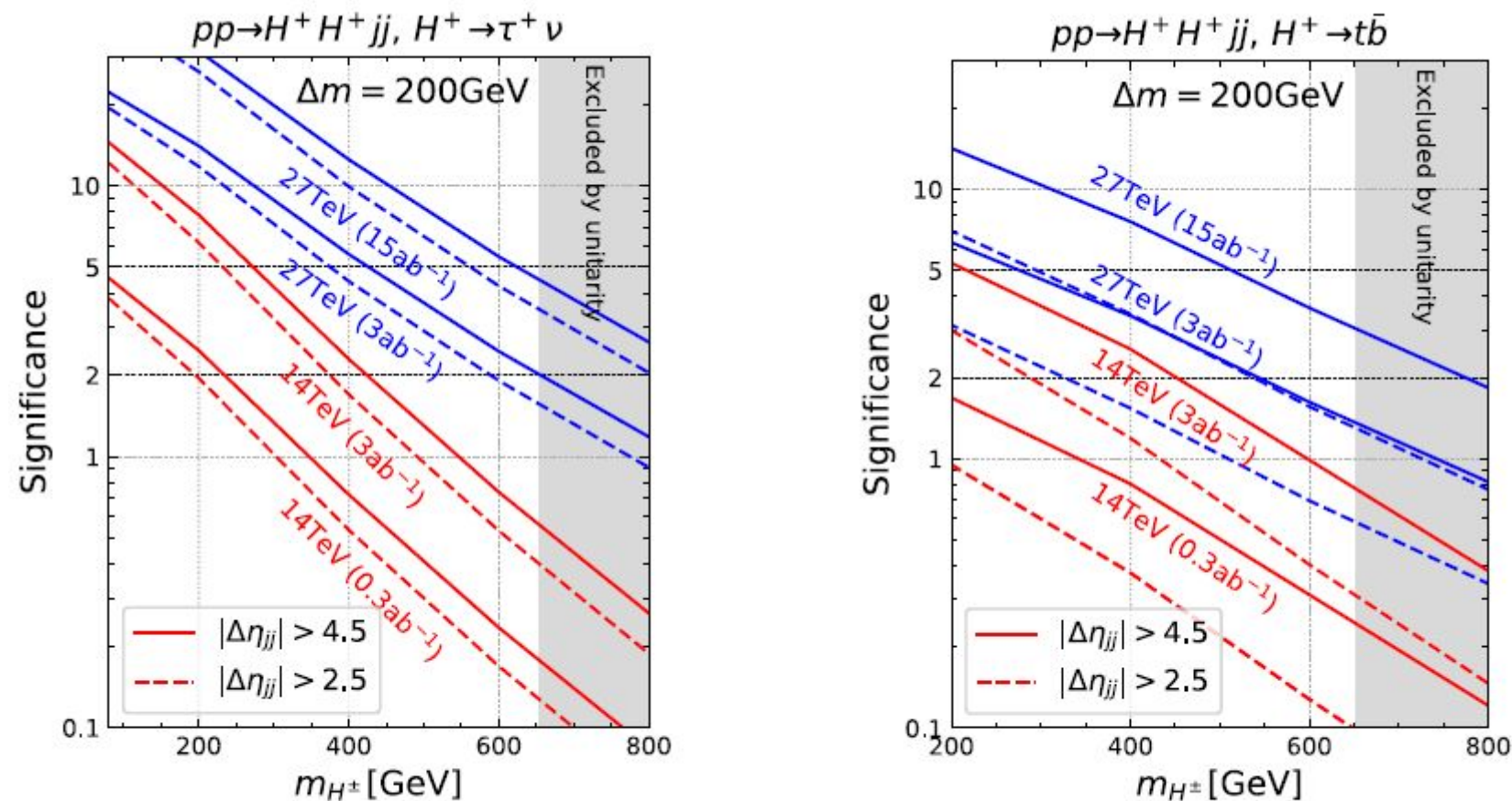


Fig. 3. Signal significance of $pp \rightarrow H^+ H^+ jj$ for $H^+ \rightarrow \tau^+ \nu$ (left) and $H^+ \rightarrow t\bar{b}$ (right).